Int. J. Solids Structures, 1969, Vol. 5, pp. 97 to 107. Pergamon Press. Printed in Great Britain

A NON-LINEAR FINITE ELEMENT ANALYSIS OF SHALLOW CIRCULAR ARCHES

A. C. WALKER

University College, London

Abstract—The large deflection behaviour of a shallow circular arch subjected to a vertical point load is studied analytically using the Rayleigh–Ritz finite element method. The energy functional employed is a little more exact than that normally used for shallow arches and the functions used in the finite element method maintain continuity up to the second derivative of the normal displacement and up to the first derivative of the tangential displacement.

The non-linear algebraic equations of equilibrium are solved to a high degree of accuracy using a Taylor's expansion technique together with the Newton–Raphson method. The stability of the symmetric deformation path is studied and a detailed analysis is carried out at the point of bifurcation on to an asymmetric deformation path. The slope of this post-buckled path is computed and is shown to be accurate for deformations well beyond the point of bifurcation.

INTRODUCTION

MOST shell structures are designed to operate such that the deformations are very small and the stresses vary linearly with the imposed loads. However, in the design of very thin shells it is important, for the rational calculations of safety factors, to explore analytically the non-linear behaviour of the shells. This is particularly necessary if there is any possibility of a loss of stability occurring along this non-linear path since a linear analysis cannot provide any indication of such an event.

The Rayleigh–Ritz finite element method [1–4] has been developed recently for use in the linear analysis of complicated shell structures. In the present paper the method is extended to non-linear analysis; and a simple shell-type structure, a shallow circular arch [5–7] is presented as an example of the use of the techniques developed herein. This structure is chosen because it is probably the simplest one which exhibits the general shell behaviour phenomena, i.e. non-linear load deflection paths, bifurcation and "snapping".

In the analysis developed here the fundamental equilibrium path emerging from the origin of zero load and zero deflection is determined using a static perturbation method [8]. This approximate path is then corrected at some load value using the Newton–Raphson technique, this corrected point is now taken as the origin for a further perturbation analysis. The stability of this fundamental path is determined and points of local maximum and minimum load are computed using the stability information. For the particular pin-ended arch considered here a point of bifurcation occurs before the first local maximum load, and for this a method [9] is outlined for obtaining numerically the value of the post-buckled slope in the "load–corresponding deflection" plot.

The most common type of loading in practice is dead loading. For a structural element subject to this loading a local maximum load will give rise to "snapping" and usually failure of the structure. Similarly the appearance of a bifurcation with a descending post-buckling slope will, for a dead-loaded structure, lead to excessively large deformations. Thus in the design process it is necessary to compute not only local maximum loads and bifurcation loads but also the post-buckled behaviour in the region of the bifurcation load.

NOTATION

E Young's modulus
P generalized load, also point load at centre of the arch
Q_i generalized coordinate
Q_c generalized coordinate corresponding to radial deflection at the centre of the arch
R arch radius
U tangential displacement of the arch middle surface
V total potential energy
W radial deflection of the arch middle surface
b arch width
e generalized displacement coordinate
q_i perturbation generalized coordinate
s perturbation parameter
t arch thickness
u non-dimensional form of the tangential displacement of the arch middle surface, $u = U/R$
w non-dimensional form of the radial displacement of the arch middle surface, $w = W/R$
α shell parameter, $\alpha = (t/R)^2/12$
β finite element constant, $\beta = m/2\phi$
ε_θ arch middle surface tangential strain
κ_θ arch middle surface curvature
ϕ half subtended angle
λ perturbation generalized load
$\Lambda, \bar{\Lambda}$ non-dimensional forms of the generalized load, $\Lambda = PR^2/EI$, $\bar{\Lambda} = \alpha\beta\Lambda$
θ angular variable
ξ non-dimensional variable

POTENTIAL ENERGY OF THE SYSTEM

The non-linear strain–displacement relationships used in this analysis are, with reference to Fig. 1,

$$\varepsilon_\theta = \frac{\mathrm{d}u}{\mathrm{d}\theta} - w + \frac{1}{2}\left(\frac{\mathrm{d}w}{\mathrm{d}\theta} + u\right)^2, \tag{1a}$$

$$\kappa_\theta = \frac{\mathrm{d}^2 w}{\mathrm{d}\theta^2} + w. \tag{1b}$$

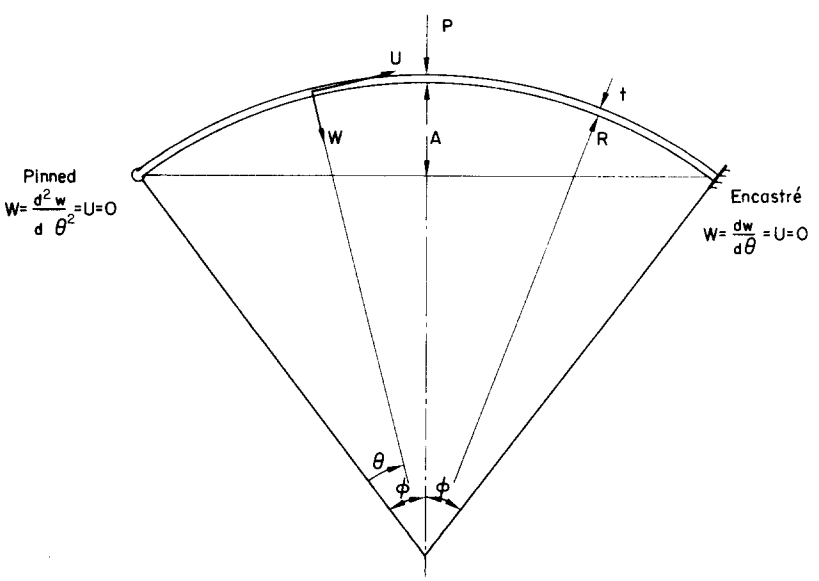

FIG. 1. Arch geometry.

These are taken from Almroth [10] and are a little more general than the corresponding Donnel shallow shell relationships.

The total potential energy of the system is given by

$$V = \frac{ERtb}{2}\int_0^{2\phi} \varepsilon_\theta^2 \, d\theta + \frac{Et^3 b}{24R}\int_0^{2\phi} \kappa_\theta^2 \, d\theta - PR[e],$$

where P is a generalized load and e is the corresponding displacement vector. The above equation may be written

$$V^* = \frac{V}{ERtb} = \frac{1}{2}\int_0^{2\phi} \varepsilon_\theta^2 \, d\theta \frac{\alpha}{2}\int_0^{2\phi} \kappa_\theta^2 \, d\theta - \alpha\Lambda[e], \tag{2}$$

where

$$\alpha = \tfrac{1}{12}(t/R)^2, \qquad \Lambda = PR^2/EI.$$

Substituting equation (1) into equation (2) and regrouping terms as

$$V^*[u, w, \Lambda] = V_2^*[u, w, \Lambda] + V_3^*[u, w] + V_4^*[u, w],$$

where V_i^* contains only ith powers of u and w, these groups are written as

$$V_2^*[u, w, \Lambda] = \frac{1}{2}\int_0^{2\phi} \left\{\left(\frac{du}{d\theta} - w\right)^2 + \alpha\left(\frac{d^2w}{d\theta^2} + w\right)^2\right\} d\theta - \alpha\Lambda[e],$$

$$V_3^*[u, w] = \frac{1}{2}\int_0^{2\phi} \left(\frac{du}{d\theta} - w\right)\left(\frac{dw}{d\theta} + u\right)^2 d\theta,$$

$$V_4^*[u, w] = \frac{1}{2}\int_0^{2\phi} \frac{1}{4}\left(\frac{dw}{d\theta} + w\right)^4 d\theta.$$

FINITE ELEMENT FORMULATION

The interval of interest ($0 \leq 0 \leq 2\phi$) is divided into m equal intervals and, with reference to Fig. 2, we may define a new non-dimensional variable ξ ($0 \leq \xi \leq 1$), such that for the nth interval the potential energy is given by

$$\beta V_{2n}^*[u_n, w_n, \bar{\Lambda}] = \frac{1}{2}\int_0^1 \{(\beta u_n' - w_n)^2 + \alpha(\beta^2 w_n'' + w_n)^2\} \, d\xi - \bar{\Lambda}[e_n], \tag{3a}$$

$$\beta V_{3n}^*[u_n, w_n] = \frac{1}{2}\int_0^1 \{(\beta u_n' - w_n)(\beta w_n' + u_n)^2\} \, d\xi, \tag{3b}$$

$$\beta V_{4n}^*[u_n, w_n] = \frac{1}{2}\int_0^1 \tfrac{1}{4}(\beta w_n' + u_n)^4 \, d\xi, \tag{3c}$$

where $w_n' \equiv dw_n/d\xi$, etc. and $\beta = m/2\phi$, $\bar{\Lambda} = \alpha\beta\Lambda$. The total potential energy of the arch comprises the sum of the potential energy of all the intervals.

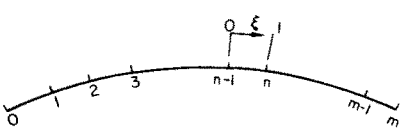

FIG. 2. Finite element configuration.

The localized Rayleigh functions describing the displacements in the nth interval are described by [13]

$$w_n = Q^1_{n-1}(1-10\xi^3+15\xi^4-6\xi^5)+Q^2_{n-1}(\xi-6\xi^3+8\xi^4-3\xi^5)+Q^3_{n-1}(\tfrac{1}{2}\xi^2-\tfrac{3}{2}\xi^3+\tfrac{3}{2}\xi^4-\tfrac{1}{2}\xi^5)$$
$$+Q^1_n(10\xi^3-15\xi^4+6\xi^5)+Q^2_n(-4\xi^3+7\xi^4-3\xi^5)+Q^3_n(\tfrac{1}{2}\xi^3-\xi^4+\tfrac{1}{2}\xi^5), \tag{4a}$$

$$u_n = Q^4_{n-1}(1-3\xi^2+2\xi^3)+Q^5_{n-1}(\xi-2\xi^2+\xi^3)+Q^4_n(3\xi^2-2\xi^3)+Q^5_n(-\xi^2+\xi^3). \tag{4b}$$

The functions (4a) maintain continuity in displacement, slope and curvature for w and Q^1, Q^2 and Q^3 are generalized coordinates specifying the magnitudes of these quantities respectively. Continuity in displacement and slope of u is specified by the functions in equation (4b) and the corresponding generalized coordinates are Q^4 and Q^5.

The algebraic equilibrium equations are obtained by substituting equation (4) into equation (3), integrating, and then differentiating with respect to each coordinate in turn. The contributions of the individual intervals are added to provide the equilibrium equations for the whole arch. The integration and differentiation processes are performed automatically and exactly on a computer thus arriving at the coefficients u_{ij}, etc. which make up the equilibrium equations,

$$u_{ij}Q_j+u_{ijk}Q_jQ_k+u_{ijkl}Q_jQ_kQ_l+\bar{\Lambda}[e_{,i}] = 0. \tag{5}$$

In equation (5) the dummy suffix summation notation is used, i.e. summations take place for repeated suffices and $0 \le i,j,k,l \le (5m-6)$, where $(5m-6)$ represents the total number of coordinates less six prescribed boundary coordinates. Also, $e_{,i} \equiv \partial e/\partial Q_i$ and since in this analysis the load is considered to be a central point load we have $e_{,i} = \delta_{ic}$ with

$$\delta_{ic} = \begin{matrix} 0 & \text{if } i \neq c \\ 1 & \text{if } i = c \end{matrix},$$

c defines the generalized coordinate corresponding to the lateral deflection of the centre of the arch.

SOLUTIONS OF EQUILIBRIUM EQUATIONS

The solution of the non-linear algebraic equilibrium equations presents many difficulties and numerous methods have been devised which may be used in conjunction with digital computers [11, 12]. Among the more popular of these methods is the Newton–Raphson iterative procedure, the use of this allows equation (5) to be solved for a particular value of $\bar{\Lambda}$, or Q_i, to any desirable degree of accuracy. One disadvantage of this method, however, is that if the initial chosen vector is too far, in the $\bar{\Lambda}-Q_i$ space, from the actual solution then the iterative procedure may not converge, or at best will converge slowly.

The method of solution presented here may be regarded as a means to providing a good initial starting vector for the Newton–Raphson procedure. However, as will be shown later, the method may also provide sufficiently accurate solutions if only moderate non-linear behaviour is to be studied.

Assume that at some values Q_i^* and $\bar{\Lambda}^*$ the equilibrium equations are completely satisfied, we may now write (see Fig. 3)

$$Q_i = Q_i^*+q_i, \qquad \bar{\Lambda} = \bar{\Lambda}^*+\lambda. \tag{6}$$

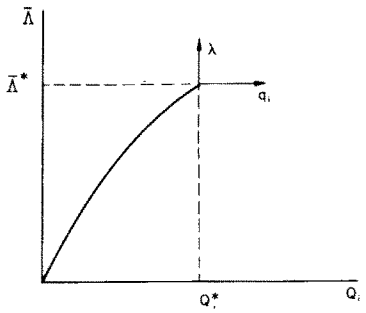

FIG. 3. Perturbation axes.

Because of the equilibrium conditions at Q_i^*, $\bar{\Lambda}^*$ the substitution of equation (6) in equation (5) gives

$$u_{ij}q_j + u_{ijk}(Q_j^*q_k + q_jQ_k^* + q_jq_k) + u_{ijkl}(Q_j^*Q_k^*q_l + q_kQ_j^*Q_l^* + Q_j^*q_kq_l + q_jQ_k^*Q_l^* + q_jQ_k^*q_l + q_iq_kQ_l^* + q_jq_kq_l) + \lambda\,\delta_{ic} = 0,$$

which can be reduced to

$$u_{ij}^*q_j + u_{ijk}^*q_jq_k + u_{ijkl}^*q_jq_kq_l + \lambda\,\delta_{ic} = 0. \tag{7}$$

we now write q_i, λ in parametric form,

$$q_i \equiv q_i(s); \qquad \lambda \equiv \lambda(s),$$

where s is some as yet undefined continuous parameter which represents progress along the desired equilibrium path. Substituting this form into equation (7) we have

$$u_{ij}^*q_j(s) + u_{ijk}^*q_j(s)q_k(s) + u_{ijkl}^*q_j(s)q_k(s)q_l(s) + \lambda(s)\,\delta_{ic} = 0. \tag{8}$$

Differentiating equation (8) with respect to s and evaluating at $q_i = \lambda = 0$ gives

$$u_{ij}^*\dot{q}_j(s) + \dot{\lambda}(s)\,\delta_{ic} = 0, \tag{9}$$

where $\dot{q}_j \equiv \partial q_j/\partial s$, etc.

Differentiating equation (8) twice with respect to s and with the results again evaluated at $q_i = \lambda = 0$, then

$$u_{ij}^*\ddot{q}_j(s) + u_{ijk}\dot{q}_j(s)\dot{q}_k(s) + \ddot{\lambda}(s)\,\delta_{ic} = 0. \tag{10}$$

The parameter s may be identified with any of the path coordinates, in this analysis it is identified with λ. Thus $\ddot{\lambda}(s) \equiv 0$ and equations (9) and (10) become

$$u_{ij}^*\dot{q}_j(\lambda) = -\delta_{ic} \tag{11}$$

$$u_{ij}^*\ddot{q}_j(\lambda) = -[u_{ijk}^*\dot{q}_j(\lambda)\dot{q}_k(\lambda)]. \tag{12}$$

From equation (11) we obtain the slopes $\dot{q}_i$ and on substitution of these into equation (12) we may, using the same matrix u_{ij}^*, obtain the curvatures $\ddot{q}_i$. This recursive process is continued by further differentiation of equation (8) and evaluation at $q_i = \lambda = 0$. When sufficient path derivatives ($\dot{q}_i$, $\ddot{q}_i$, etc.) have been obtained the path itself may be synthesized from

$$Q_i = Q_i^* + q_i\lambda + \tfrac{1}{2}\ddot{q}_i\lambda^2 + \tfrac{1}{6}\dddot{q}_i\lambda^3 + \ldots, \tag{13a}$$

$$\bar{\Lambda} = \bar{\Lambda}^* + \lambda. \tag{13b}$$

If a value λ^0 is substituted in equation (13) a set of values $(Q_i^0, \bar{\Lambda}^0)$ is obtained which only approximately satisfies equation (5). A more exact solution at Λ^0 is obtained by using the Newton–Raphson iterative procedure. Thus, we obtain corrections $(\delta q_i)_{t+1}$ at iterative cycle t from the equations

$$\begin{aligned}(\delta q_i)_{t+1} &= -[\bar{u}_{ij}]_t^{-1} \cdot [u_{ij}(Q_j)_t + u_{ijk}(Q_j)_t(Q_k)_t + u_{ijkl}(Q_j)_t(Q_k)_t(Q_l)_t + \bar{\Lambda}^0 \delta_{ic}], \\ (Q_i)_{t+1} &= (Q_i)_t + (\delta q_i)_{t+1}.\end{aligned} \tag{14}$$

In equation (14) $\bar{u}_{ij}$ is formed in the same way as u_{ij}^* in equation (7) but with values of $(Q_j)_t$ corresponding to Q_j^*. As the values Q_i^0 and $\bar{\Lambda}^0$ obtained from the Taylor's expansion will be close to the exact values, the number of Newton–Raphson iterations is very small. When the residual error (usually $\sum_{i=0,1}^{(5m-1)} (\delta q_i)_{t+1}^2$) falls below a specified value the Taylor's expansion technique may be commenced anew.

STABILITY ANALYSIS

A change of stability along an equilibrium path is marked by the vanishing of the second variation of the potential energy. In the term of the method of analysis used here this signifies the determinant of the matrix u_{ij}^* of equation (7) becoming zero. The following is a procedure which may be used to determine the value of the load, Λ_{crit}, at which a loss of stability occurs and also to determine the behaviour of the structure in the immediate post-buckled region.

At $Q_i = Q_i^*$ and $\bar{\Lambda} = \bar{\Lambda}^*$, $(\bar{\Lambda}^* < \bar{\Lambda}_{\text{crit}})$ we assume that equilibrium equation (5) have been completely satisfied. Hence

$$u_{ij}Q_j^* + u_{ijk}Q_j^*Q_k^* + u_{ijkl}Q_j^*Q_k^*Q_l^* - \Lambda^* \delta_{ic} = 0,$$

also we assume that a Taylor's expansion with respect to $\bar{\Lambda}$ has been performed so that the fundamental path is adequately described by

$$\begin{aligned}{}^F Q_i(\Lambda) &= Q_i^* + \left.\frac{\partial Q_i}{\partial \bar{\Lambda}}\right|_{Q_i = Q_i^*} \lambda + \frac{1}{2}\left.\frac{\partial^2 Q_i}{\partial \bar{\Lambda}^2}\right|_{Q_i = Q_i^*} \lambda^2 + \ldots \\ &= Q_i^* + S_i\lambda + T_i\lambda^2 + \ldots, \end{aligned} \tag{15a}$$

$$\bar{\Lambda} = \bar{\Lambda}^* + \lambda. \tag{15b}$$

The post buckled path is now described by

$$Q_i = {}^F Q_i(\bar{\Lambda}) + q_i.$$

Equations (15) are substituted into the energy functions and since the post-buckled path is in equilibrium the appropriate equilibrium equations are obtained by differentiating this energy function with respect to q_i. After deletion of those terms which collectively satisfy the equilibrium conditions (equation (5)) for the fundamental path the resulting equations for the post-buckled path are

$$\begin{aligned}&u_{ij}q_j + u_{ijk}[{}^F Q_j(\bar{\Lambda})q_k + q_j {}^F Q_k(\bar{\Lambda}) + q_j q_k] + u_{ijkl}[{}^F Q_j(\bar{\Lambda}) {}^F Q_k(\bar{\Lambda}) q_l + {}^F Q_j(\Lambda) q_k {}^F Q_l(\bar{\Lambda}) \\ &\quad + q_j {}^F Q_k(\bar{\Lambda}) {}^F Q_l(\bar{\Lambda}) + {}^F Q_j(\bar{\Lambda}) q_k q_l + q_j {}^F Q_k(\bar{\Lambda}) q_l + q_j q_k {}^F Q_l(\bar{\Lambda}) + q_j q_k q_l] = 0. \end{aligned} \tag{16}$$

Once more we write q_i, λ in parametric form

$$q_i \equiv q_i(s); \qquad \lambda \equiv \lambda(s).$$

Differentiating equation (16) and evaluating at $q_i = 0$ gives

$$u_{ij}\dot{q}_j + u_{ijk}[{}^FQ_j(\bar{\Lambda})\dot{q}_k + {}^FQ_k(\bar{\Lambda})\dot{q}_j] + u_{ijkl}[{}^FQ_j(\bar{\Lambda}){}^FQ_k(\bar{\Lambda})\dot{q}_l + {}^FQ_j(\bar{\Lambda})\dot{q}_k{}^FQ_l(\Lambda) + \dot{q}_j{}^FQ_k(\bar{\Lambda}){}^FQ_l(\bar{\Lambda})] = 0,$$

which may be written

$$[u_{ij} + \bar{u}_{ij}(\bar{\Lambda})]\dot{q}_j = 0, \tag{16a}$$

where $\bar{u}_{ij}$ is a function of $\bar{\Lambda}$. At the bifurcation load we have

$$|u_{ij} + u_{ij}(\bar{\Lambda}_{\text{crit}})| = 0,$$

yielding the critical load, Λ_{crit}. Also, if s is identified with one of the generalized coordinates, say q_s (in this analysis it was identified with the central slope), then at $\bar{\Lambda} = \Lambda_{\text{crit}}$ equations (16a) are normalized with respect to q_s and the reduced equations may be solved to give $\dot{q}_j$ $(j \neq s)$, $\dot{q}_s = 1$. Differentiating equation (16) twice with respect to s and evaluating at $q_i = 0$ yields

$$u_{ij}\ddot{q}_j + u_{ijk}[{}^FQ_j\ddot{q}_k + {}^FQ_k\ddot{q}_j] + u_{ijkl}[{}^FQ_j{}^FQ_k\ddot{q}_l + {}^FQ_j\ddot{q}_k{}^FQ_l + \ddot{q}_j{}^FQ_k{}^FQ_l] + 2\dot{\lambda}\{u_{ijk}[{}^FQ'_j\dot{q}_k + {}^FQ'_k\dot{q}_j] + u_{ijkl}[{}^FQ'_j{}^FQ_k\dot{q}_l + {}^FQ_j{}^FQ'_k\dot{q}_l + {}^FQ'_j\dot{q}_k{}^FQ_l + {}^FQ_j\dot{q}_k{}^FQ'_l + \dot{q}_j{}^FQ'_k{}^FQ_l + \dot{q}_j{}^FQ_k{}^FQ'_l]\} + 2\{u_{ijk}[\dot{q}_j\dot{q}_k] + u_{ijkl}[{}^FQ_j\dot{q}_k\dot{q}_l + \dot{q}_j{}^FQ_k\dot{q}_l + \dot{q}_j\dot{q}_k{}^FQ_l]\} = 0,$$

where ${}^FQ'_i \equiv \partial {}^FQ_i/\partial\lambda$ and ${}^FQ_j, {}^FQ'_j$ are evaluated at $\bar{\Lambda}_{\text{crit}}$. The above equation may be reduced to

$$[u_{ij} + \bar{u}_{ij}(\bar{\Lambda}_{\text{crit}})]\ddot{q}_j + 2(\dot{\lambda}\bar{u} + \bar{\bar{u}}_i) = 0. \tag{17}$$

Multiplying each equation by $\dot{q}_i$ and adding gives

$$\dot{\lambda}\Big|_{\bar{\Lambda}=\bar{\Lambda}_{\text{crit}}} = -\frac{\bar{\bar{u}}_i\dot{q}_i}{\bar{u}_i\dot{q}_i}.$$

If now $\dot{\lambda}$ is substituted in equation (17) we may solve the reduced equations to give $\ddot{q}_j$ $(j \neq s)$, $\ddot{q}_s = 0$.

This process is continued by differentiating equation (16) three times with respect to q_s and evaluating at $q_i = 0$. When the necessary substitutions of $\dot{\lambda}$, $\dot{q}_i$, $\ddot{q}_i$ are made we may obtain $\dddot{\lambda}$ and $\dddot{q}_i$ $(i \neq s)$.

To determine the post-buckled behaviour of the structure we may now synthesize the plot of load vs. corresponding deflection $(\bar{\Lambda} - Q_c)$ from the computed path derivatives, $\dot{\lambda}$, $\dot{q}_i$, etc.

Now

$$\frac{\partial Q_c}{\partial\lambda} = \frac{(\partial Q_c/\partial q_s)}{(\partial\lambda/\partial q_s)},$$

but

$$Q_c = {}^FQ_c + q_c,$$

therefore

$$\frac{\partial Q_c}{\partial q_s} = {}^{F}Q_c' \cdot \frac{\partial \lambda}{\partial q_s} + \frac{\partial q_c}{\partial q_s}.$$

Hence,

$$\left(\frac{\partial Q_c}{\partial \lambda}\right)_{\bar{\Lambda}=\bar{\Lambda}_{crit}} = [{}^{F}Q_c' + (\dot{q}_c/\dot{\lambda})]\Big|_{\bar{\Lambda}=\bar{\Lambda}_{crit}},$$

where from computations $\dot{q}_c = \dot{\lambda} = 0$ at $\bar{\Lambda} = \bar{\Lambda}_{crit}$. Thus as expected [9] and as shown in Fig. 4 a first order perturbation analysis at the bifurcation load yields no information on the post-buckling path in the $\bar{\Lambda} - Q_c$ plot. The second order perturbation, however, yields

$$\left(\frac{\partial Q_c}{\partial \lambda}\right)_{\bar{\Lambda}=\bar{\Lambda}_{crit}} = \left(\frac{\ddot{\lambda}}{{}^{F}Q_c'\ddot{\lambda} + \ddot{q}_c}\right)\Big|_{\bar{\Lambda}=\bar{\Lambda}_{crit}}.$$

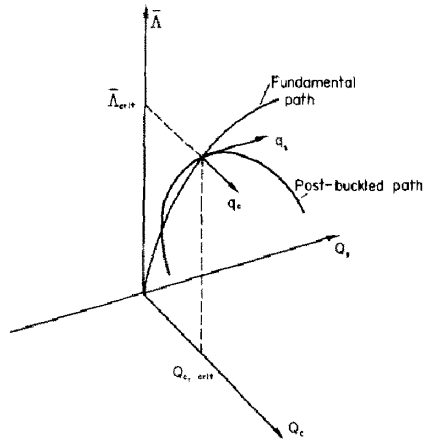

FIG. 4. Bifurcation.

Thus we may construct the immediate post-buckled path using

$$Q_c = Q_c\Big|_{\Lambda=\Lambda_{crit}} + \frac{\partial Q_c}{\partial \lambda}\Big|_{\Lambda>\Lambda_{crit}} (\lambda - \lambda_{crit}).$$

Similarly the other post-buckled path coordinates may be determined and, if necessary, the equilibrium path remote from the buckled region may be determined using the Taylor's expansion–Newton–Raphson method described in the previous section.

The local maximum load may be obtained in a similar manner to that outlined above for the bifurcation load.

DISCUSSION

The power of the finite element method is best seen when it is applied to problems of structures having complicated loading and geometry. However, the example presented here of a circular arch, $R/t = 500$, $\phi = 10°$, loaded centrally by a point load serves perfectly well to illustrate the application of the general computational method presented above.

The fundamental path is given in Fig. 5 for a pin-ended arch and in Fig. 6 for an encastré arch. It may be seen from these that the Taylor's expansion about the origin gives satisfactory accuracy well into the non-linear range of deformation. The number of itera-

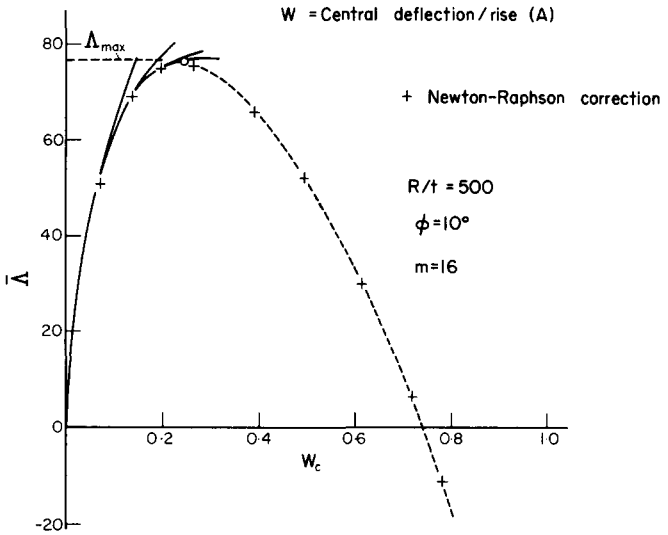

FIG. 5. Arch fundamental path.

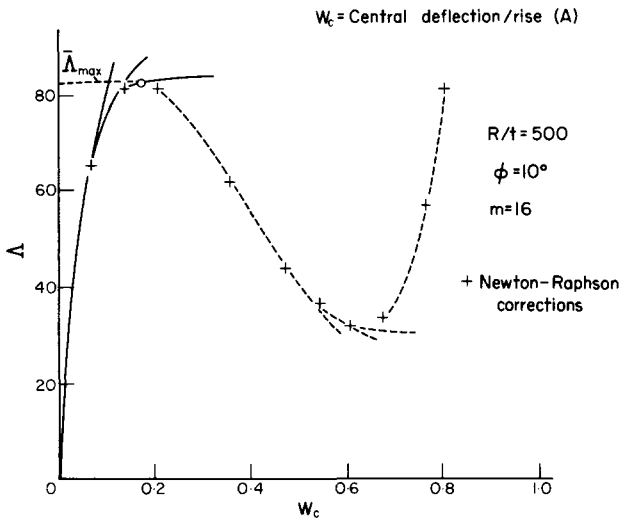

FIG. 6. Encastré arch fundamental path.

tions required by the Newton–Raphson method was never more than two, the central deflection was taken as the prescribed generalized coordinate for this part of the computation. In Table 1 convergence of the features of the results with increasing number of

TABLE 1

m	$\bar{\Lambda}_{max}$	$\bar{\Lambda}_{crit}$	$\partial\bar{\Lambda}/\partial w_c$
6	78·92	66·63	−119·2
8	76·72	66·22	−115·4
12	76·27	66·09	−114.4
16	76·21	66·08	−113·1

elements is presented. It is evident from these that even the coarsest interval provides sufficient accuracy for practical design calculations and as is seen from Fig. 7 the slope of the post-buckling path determines accurately the behaviour of the structure at load values remote from the buckling load.

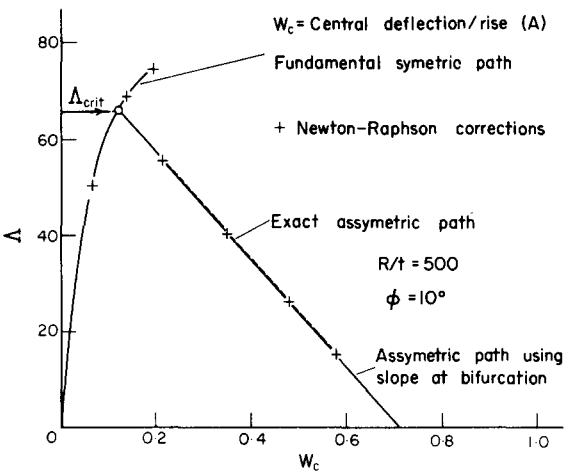

FIG. 7. Pinned arch bifurcation and post-buckled path.

Acknowledgements—The author wishes to acknowledge his indebtedness to Mr. D. G. Hall for his aid in programming this problem.

REFERENCES

[1] O. C. ZIENKIEWICZ, *The Finite Element Method in Structural and Continuum Mechanics*. McGraw-Hill (1967).
[2] *Proc. Conf. on Matrix Methods in Structural Mechanics*, Wright-Patterson Air Force Base, Ohio, 1965. AFF-TR-66-80.
[3] D. R. NAVARATNA, T. H. H. PIAN, and E. A. WITMER, Stability analysis of shells of revolutions by the finite element method. *AIAA Jnl* **6**, 355 (1968).
[4] J. M. T. THOMPSON, Localised Rayleigh functions for structural and stress analysis. *Int. J. Solids Struct.* **3**, 285 (1967).
[5] Y. C. FUNG and A. KAPLAN, Buckling of low arches as curved beams of small curvature. *NACA tech. Note* 2840 (1952).
[6] H. L. SCHREYER and E. F. MASUR, Buckling of shallow arches. *J. Engng Mech. Div. Am. Soc. civ. Engrs* **92**, EM4 (Aug. 1966).
[7] A. GJELSVIK and S. R. BODNER, Energy criterion and snap buckling of arches. *J. Engng Mech. Div. Am. Soc. civ. Engrs* **88**, EM5 (Oct. 1962).
[8] J. M. T. THOMPSON and A. C. WALKER, The non-linear perturbation analysis of discrete structural systems. *Int. J. Solids Struct.* **4**, 757 (1968).

[9] J. M. T. THOMPSON and A. C. WALKER, A general theory for the branching analysis of discrete structural systems. *Int. J. Solids Struct.* To be published.
[10] B. O. ALMROTH, Buckling of a cylindrical shell subjected to nonuniform external pressure. *J. appl. Mech.* **29**, 675 (1962).
[11] H. A. SPANG, A review of minimisation techniques for non linear functions. *J. Soc. ind. appl. Math.* **4**, 543 (1962).
[12] K. L. REMMLER, D. W. CAWOOD and J. A. STANTON, Solution of systems of non-linear equations. Lockheed MSC/HREC, NASA 8-20178 (Oct. 1966).
[13] A. C. WALKER, Rayleigh–Ritz method for plate flexure. *J. Engng Mech. Div. Am. Soc. civ. Engrs* **93**, EM6 p. 139 (1967).

(*Received* 29 *April* 1968)

Абстракт—Исследуется аналитически поведение при больших изгибах круглой, пологой арки подверженной сосредоточенной, вертикальной нагрузке, используя метод Рэлея—Ритца конечного элемента. Применяется более точно функционал энергии, чем нормально это делается для пологих арок. Функции, использованные в методе конечного элемента, остаются непрерывными до второй производной нормаьного перемещения включительно и до первой производной тангенциального перемещения, также, включительно. Решаются нелинейные алгебраические уравнения равновесия с большой степенью точности, используя метод разложения Тейлора в месте с методом Ньютона-Рафсона. Исследуется устойчивость асимметрической ветви деформации. Приводится детальный анализ при точке бифуркации в направлении несимметрической ветви деформации. Решается наклон этой ветви после выпучивания и показывается, что она справедлива для деформаций на некотором расстоянии от точки бифуркации.